Polymer Bulletin
https://doi.org/10.1007/s00289-023-04788-4

ORIGINAL PAPER

Fascinating study of elastic, FTIR, and antimicrobial properties of silver nanochromite at different annealing temperatures

W. M. Gamal[1] · Asmaa A. H. El-Bassuony[1] · H. K. Abdelsalam[2]

Received: 15 September 2022 / Revised: 5 March 2023 / Accepted: 3 April 2023

Abstract

In this work, $Ag_{0.5}Cr_{2.5}O_4$ nanochromite is fabricated utilizing a simple process (flash technique) at various annealing temperatures (room and 900 °C). The particle sizes of the materials under study were shown to be in the nanoscale range by atomic force microscopy (AFM) and field emission scanning electron microscopy (FESEM). Fourier transform infrared (FTIR) analysis was performed to verify the fabrication of the examined nanosamples and evaluate the bands behavior. The tetrahedral A-site (622.9 cm^{-1} for room temperature, 630.6 cm^{-1} for 900 °C) and the octahedral B-site (557.3 cm^{-1} for room temperature, 563.1 cm^{-1} for 900 °C) were the two prominent bands measured by FTIR analysis. The elastic characteristics of $Ag_{0.5}Cr_{2.5}O_4$ nanoparticles were examined using FTIR measurements, revealing that the interatomic bonding of the atoms at 900 °C is higher than at room temperature. In addition, the elastic characteristics may be understood by analyzing the transverse and longitudinal velocities. Both Gram-positive and Gram-negative bacteria were effectively inhibited by the samples evaluated for antibacterial properties; however, neither sample showed any antifungal activity. Therefore, it is highly suggested that the investigated samples could be used in different applications, particularly biological ones.

Keywords Nanochromite · AFM · FTIR · Elastic properties · Antimicrobial application

✉ Asmaa A. H. El-Bassuony
asmaa@sci.cu.edu.eg; asmaa.ali@cu.edu.eg

[1] Physics Department, Faculty of Science, Cairo University, Giza, Egypt

[2] Basic Science Department, Higher Institute of Applied Arts 5Th Settlement, New Cairo, Egypt

Published online: 18 April 2023

Introduction

Silver is an example of a noble metal used in several industries, including electrical, water treatment, antiviral/antibacterial research, and solar cell manufacturing [1–5]. Nanochromites are very stable at high annealing temperatures, making them suitable for various technological uses [6]. The study of the physical characteristics of nanoparticles is vital for elucidating the sample's behavior and determining the most appropriate use for the sample [7–10]. Selecting the best technique for improving products is essential. In this research, nanoparticles were created using a flash auto-combustion technique for excellent stoichiometric regulation. In addition, it is a simple, low-cost, and quick procedure that saves time [6, 11]. The recent irresponsible overuse of antibiotics has increased the urgency of finding effective alternatives, leading to the rise in the popularity of silver complexes and other antimicrobial applications [12–15]. Therefore, an antibacterial study used both Gram-positive and Gram-negative bacteria in addition to fungi for testing.

X-ray examination of $Ag_{0.5}Cr_{2.5}O_4$ nanoparticles at room temperature and 900 °C revealed a cubic structure, as described in our previous work [16, 17]. The nature of the binding forces in solids may be elucidated by measuring elastic constants such as Poisson's ratio, Young's modulus, rigidity, and bulk modulus. FTIR analysis may be used to learn about elastic properties, and it can reveal the Debye temperature and the longitudinal velocity, among other elastic constants. Moreover, the X-ray diffraction pattern parameters, combined with those of FTIR spectroscopy, are significant when calculating certain elastic moduli, such as shear and sound velocities [18, 19]. This enables the measurement of elastic characteristics to estimate the interatomic bonding strength. According to the authors' knowledge, no previous study has been conducted on the elastic properties of $Ag_{0.5}Cr_{2.5}O_4$ nanochromite. It is reported from our previous work that silver chromite with the chemical formula $Ag_2Cr_2O_4$ nanoparticles with the ratio of Ag/Cr ion (1:1) at room temperature is stronger than $Ag_2Fe_2O_4$ nanoparticles with the ratio of Ag/Fe ion (1:1) [20]. Also, when comparing silver chromite with different chemical formulas $AgCrO_2$ with the ratio of Ag/Cr ion (1:1) at room temperature gave high strength than $AgFeO_2$ with the ratio of Ag/Fe ion (1:1) [21]. This indicates that chromium ions possess more elasticity than iron ions, which could be used in various applications. The author chose to add chromium to silver over iron because chromium's elasticity is higher than iron's. The authors decided to increase the ratio of chromium to silver by 5:1 to ensure that when the element of chromium is increased over iron, the elasticity will increase, and this has already been confirmed in this research. The authors also studied the mechanical properties of the investigated material with increasing temperature. Thus, the authors study the mechanical properties of silver chromite by increasing the chromite concentration ($Cr_{2.5}$) at the expense of decreasing silver ion concentration ($Ag_{0.5}$) with the ratio of Ag/Cr ion (1:5) compared with previous work ($Ag_2Cr_2O_4$ and $AgCrO_2$) with the ratio of Ag/Cr (1:1) [20, 21]. Moreover, the authors studied the effect of the investigated samples with various temperatures, and they found that by increasing the annealing temperature, the elasticity of the nanosample increased.

Consequently, this research aims to explore the FTIR analysis of $Ag_{0.5}Cr_{2.5}O_4$ nanochromite, the elastic properties derived from infrared analysis at various annealing temperatures, and the antibacterial application of the investigated materials. The study of the elastic properties of the investigated samples is novel, and this is the first time to illustrate the mechanical properties of $Ag_{0.5}Cr_{2.5}O_4$ nanoparticles at different annealing temperatures from FTIR analysis. An illustration of elastic properties can give a complete description of the samples that could be appropriately used in many technological applications.

Experimental approaches

Preparation and analysis

Nanochromite ($Ag_{0.5}Cr_{2.5}O_4$) was synthesized by a simple technique (flash technique). Nitrate salts, such as chromium nitrate (100.04 g Cr $(NO_3)_3$) and silver nitrate (8.49 g $AgNO_3$), are the starting materials. Urea (20 g) and some distilled water were added to the mixture, as shown in Fig. 1. The mixture is then heated to 250 °C to become a powder. The powder used in the analyses was annealed for 2 hours at two different temperatures (room temperature and 900 °C) as the last stage in this experiment. The FTIR (Fourier transform infrared) analysis was performed between 400 and 4000 cm^{-1} using a spectrometer manufactured in Japan called a Jasco FTIR 300 E. The Wet-PM-9600, a Japanese-made atomic force microscopy instrument, was used at room temperature to take the measurements in a non-contact mode. The field emission scanning electron microscopy (FESM) was measured using a 250 FEG quanta model.

Antimicrobial measurement

The Kirby-Bauer technique [22] with a modified disk was used for the in vitro examination of the antibacterial activity. *Staphylococcus aureus* ATCC 12,600, *Bacillus subtilis* ATCC 6051, and *Streptococcus faecalis* ATCC 19,433 were Gram-positive bacteria strains examined and analyzed. The Gram-negative bacteria tested were *Pseudomonas aeruginosa* ATCC 10,145, *Escherichia coli* ATCC 11,775, and *Neisseria gonorrhea* ATCC 19,424. *Candida albicans* ATCC 7102 and *Aspergillus flavus* link were also tested for their fungal properties. The nanosample $Ag_{0.5}Cr_{2.5}O_4$ was used against the tested bacteria and fungi. A 100 µl of tested bacteria or fungi were spread on the agar surface to form a colony, and then the investigated sample was added to it. The Petri plates were cultured at 30° C for 24 and 48 h. The inhibition zone diameters were measured to assess the efficacy of the substances tested against the bacteria and fungi utilized in the experiment. *Ampicillin* and *Amphotericin B* were considered as antibacterial and antifungal control to be compared with them.

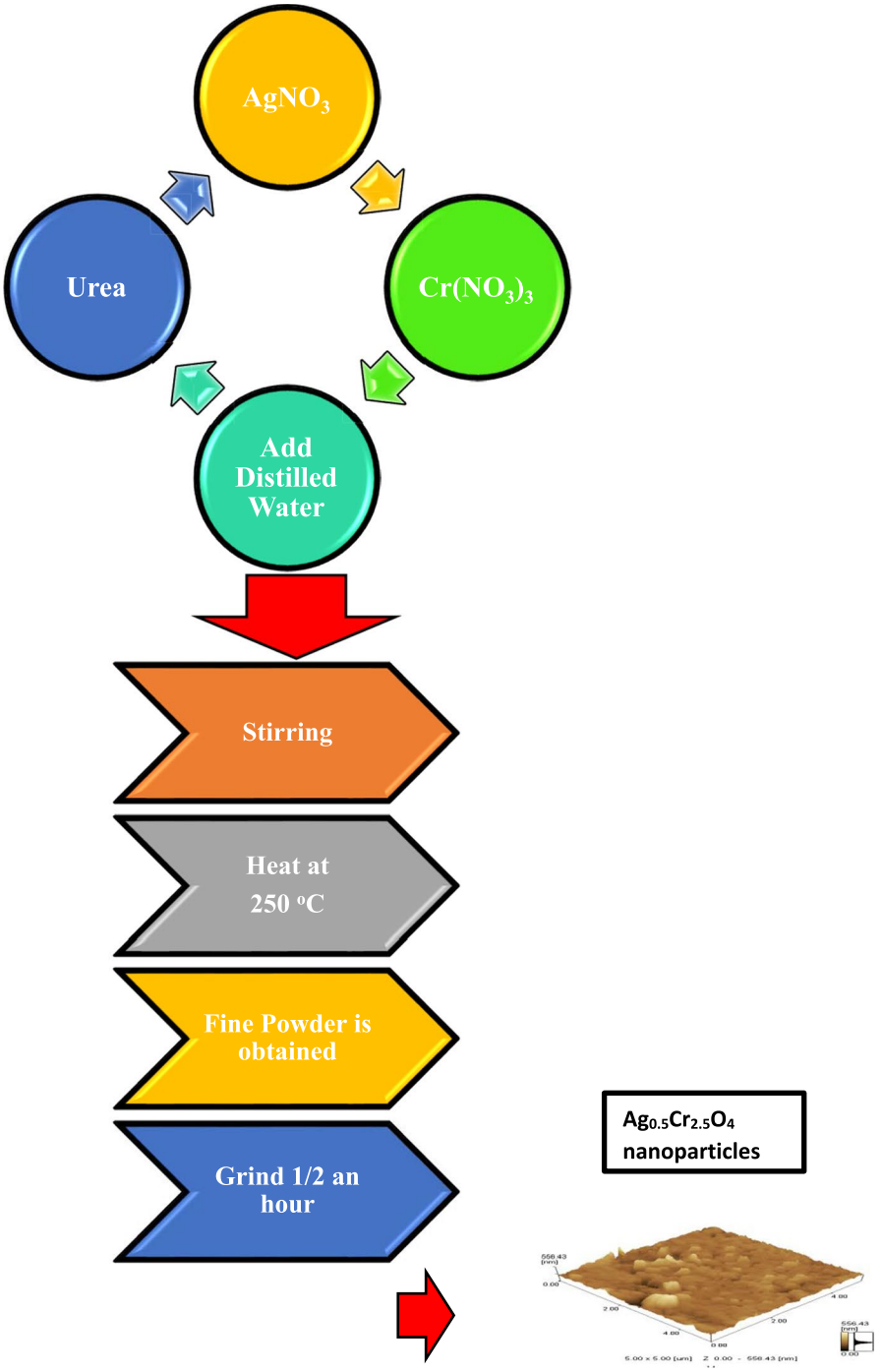

Fig. 1 Preparation method of $Ag_{0.5}Cr_{2.5}O_4$ at room temperature and 900 °C

Results and discussion

AFM study

Figure 2a–c shows the atomic force microscopy (AFM) study of the surface morphology of $Ag_{0.5}Cr_{2.5}O_4$ nanoparticles at 900 °C. The figures show that agglomeration occurred in the tested sample due to no surfactant used during the preparation of the nanoparticles [23, 24], as shown in Fig. 2a. Table 1 shows the values of the particle size and roughness. The AFM micrograph was analyzed using the image editing tool ImageJ to generate the average particle size histogram and a roughness histogram, as shown in Fig. 2b, c, respectively. Finally, the average particle sizes of the examined samples were found to be on the nanoscale.

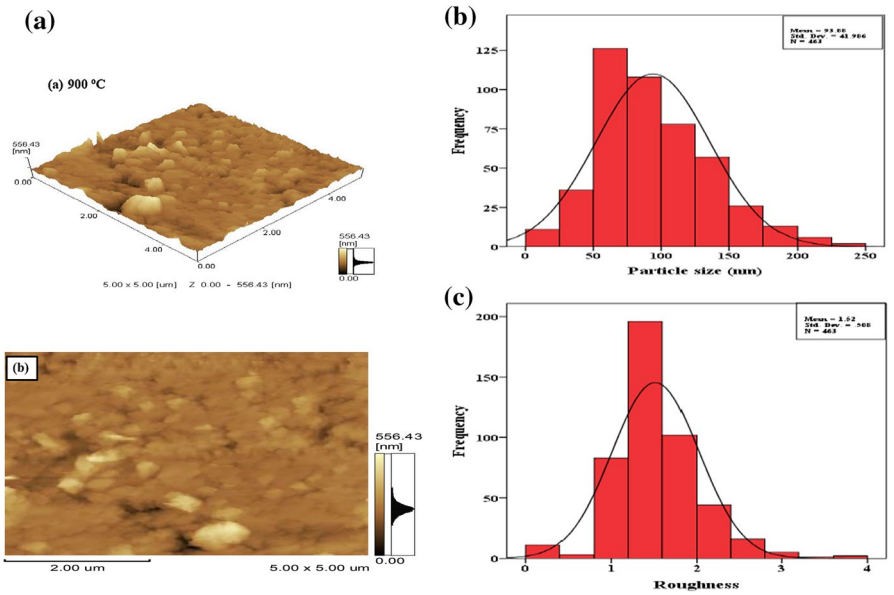

Fig. 2 **a** 3D, **b** plane image of Atomic Force Microscopy (AFM) of $Ag_{0.5}Cr_{2.5}O_4$ at 900 °C. **b** The histogram of the average particle size estimated from AFM of $Ag_{0.5}Cr_{2.5}O_4$ at 900 °C. **c** The histogram of the roughness estimated from AFM of $Ag_{0.5}Cr_{2.5}O_4$ at 900 °C

Table 1 The values of the molecular weight M, crystallite size from XRD, particle size from AFM, particle size from FESEM, and roughness of $Ag_{0.5}Cr_{2.5}O_4$ at room temperature and 900 °C

Samples	*M*	Crystallite size XRD (nm) [16, 17]	Particle size AFM (nm)	Particle size FESEM (nm)	Roughness (μm)
Room	247.922	72.61	–	79.9	–
900 °C		47.9	93.9	65.1	1.52

FESEM and EDX study

Figure 3a, b shows the field emission scanning electron microscopy (FESEM) study of the investigated samples at various annealing temperatures. Table 1 shows that the particle size of both samples estimated from the FESEM image was in the nanoscale range. The agglomeration appears in Fig. 3a, b, especially at $Ag_{0.5}Cr_{2.5}O_4$ nanoparticles at 900 °C, since the surfactant was not added during the synthesis of the samples [25]. Thus, the FESEM test assured the nanoscale range of the investigated samples.

Figure 3c and Table 2 show energy-dispersive X-ray analysis (EDX) of $Ag_{0.5}Cr_{2.5}O_4$ nanoparticles at room temperature. The values showed the homogeneity mixing of Ag, O, and Cr atoms. Moreover, there is a good agreement between theoretical and experimental composition values of weight percentage (wt%) and atomic percentage (at.%) of the investigated sample.

FTIR Study

In general, in solids, ion vibrations in the crystal lattice are attributed to infrared bands [26]. Fourier transform infrared spectroscopy (FTIR) is utilized to examine the structural modifications of $Ag_{0.5}Cr_{2.5}O_4$ nanoparticles at room temperature and 900 °C in the wave number range of 400–4000 cm^{-1}, as shown in Fig. 4 and Table 3. One of the primary strong absorption bands in the FTIR spectra of both materials is at approximately 500 cm^{-1} (peak 1), while the other is at around 600 cm^{-1} (peak 2). The shorter distance between Cr^{3+} and O^{2-} atoms in octahedral complexes, relative to tetrahedral complexes [27–30], may account for the observed band position differences. As the annealing temperature is raised, the crystallinity is improved. The tetrahedral absorption peak of the $Ag_{0.5}Cr_{2.5}O_4$ nanoparticle at 900 °C shifts slightly toward the higher frequency side relative to that at room temperature. The C–O–C asymmetric stretching vibration causes the spectral peak at location (3). The band at peak (4) suggests that C=C stretching vibration occurs. The stretching vibration of the C=O and carboxyl groups may also be responsible for the band at peak 5. The band at peak (6) is assumed to be generated by the absorption of atmospheric CO_2 on the surface of the nanoparticles during the FTIR test. The band at peak (7) may be related to the stretching vibration of the C–H group. The strong band at peak (8) may be attributed to water symmetric stretching vibration and NH group.

Elastic Study

Elastic constants are essential in measuring the resistance of a crystal to an externally applied stress. Thus, the elastic properties of nanoparticles play an essential role in industrial applications [26, 31]. FTIR analysis was used to examine the elastic properties of $Ag_{0.5}Cr_{2.5}O_4$ nanoparticles at room temperature and 900 °C, as reported by

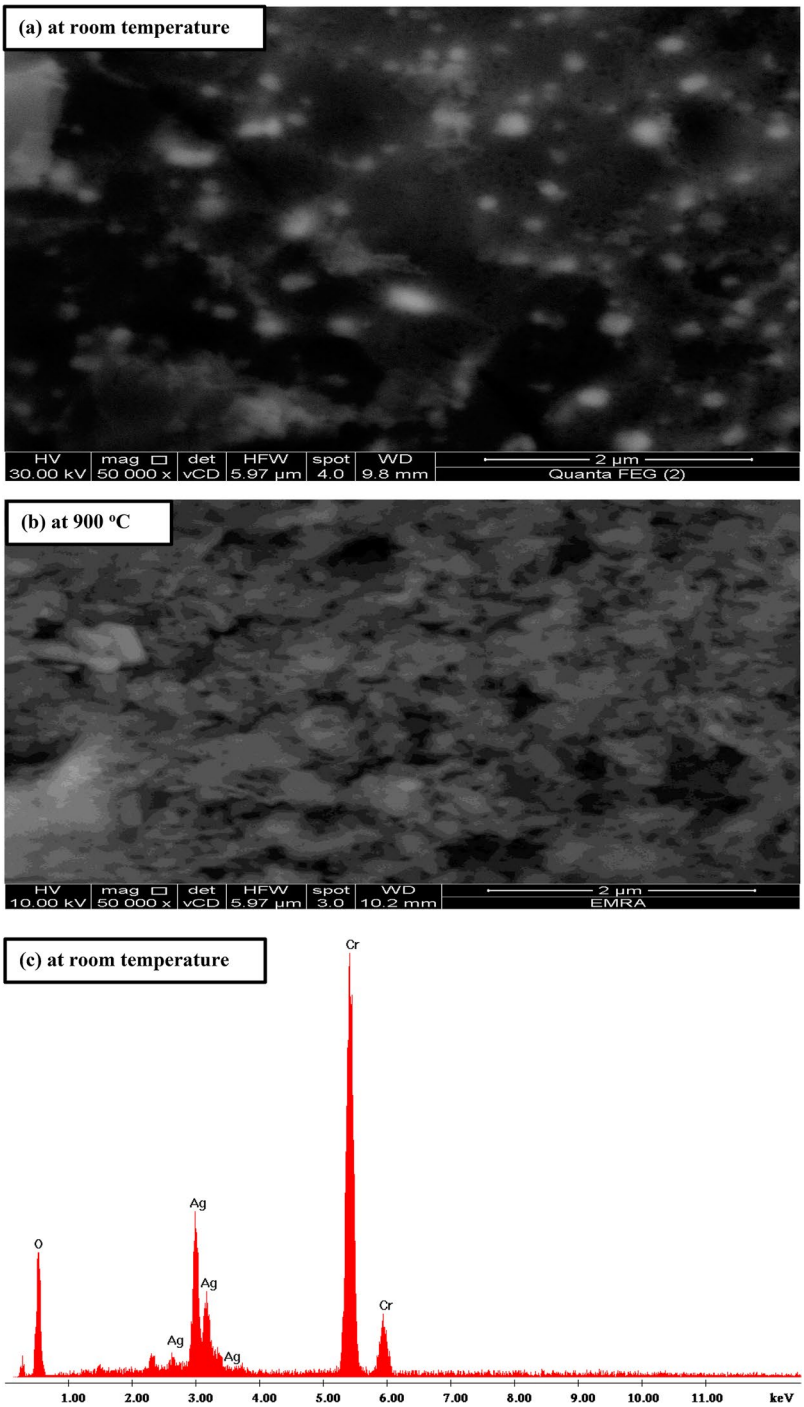

Fig. 3 FESEM microscopy of $Ag_{0.5}Cr_{2.5}O_4$ at **a** room temperature, **b** 900 °C, **c** EDX analysis of $Ag_{0.5}Cr_{2.5}O_4$ at room temperature

Table 2 EDX analysis of $Ag_{0.5}Cr_{2.5}O_4$ at room temperature

Elements	Weight percentage (wt%)		Atomic percentage (at.%)	
	Theoretical	From EDX analysis	Theoretical	From EDX analysis
Ag L	21.8	23.8	7.1	7.7
Cr K	52.4	49.2	35.7	33.1
O K	25.8	27.1	57.1	59.2

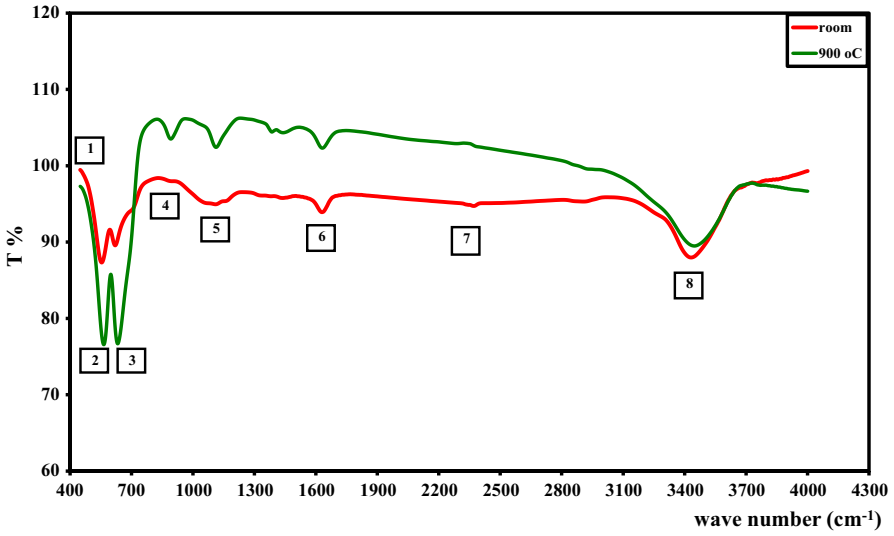

Fig. 4 FTIR spectra of $Ag_{0.5}Cr_{2.5}O_4$ at room temperature and 900 °C

Table 3 FTIR peaks of $Ag_{0.5}Cr_{2.5}O_4$ at room temperature and 900 °C

No. of Peaks	1	2	3	4	5	6	7	8
Room	557.327	622.895	888.059	1435.74	1629.55	2367.19	2914.88	3430.74
900 °C	563.112	630.609	891.916	1114.65	1631.48	2374.91	–	3434.6

Modi et al. [31]. The tetrahedral and octahedral force constants, K_t and K_o, were calculated by the following equations [28]:

$$K_t = 7.62 \times M_A \times \nu_1^2 \times 10^{-7} \mathrm{N/m} \quad (1)$$

$$K_o = 10.62 \times \frac{M_B}{2} \times \nu_2^2 \times 10^{-7}\ \mathrm{N/m} \quad (2)$$

Table 4 Elastic parameters of $Ag_{0.5}Cr_{2.5}O_4$ at room temperature and 900 °C

Samples	$\nu 1$ tetra × 102 (m^{-1})	$\nu 2$ octa × 102 (m^{-1})	MA × 103	MB × 103	a (Å)	Dx Kg/m3	Kt (N/m)	Ko (N/m)	K (N/m)	νav × 102 (m^{-1})	θD (K)	$C11$ (Gpa)
Room	622.895	557.327	102.281	109.579	8.254	9250	302.398	180.735	241.567	59,011.1	13,522.2	292.7
900 °C	630.609	563.112	96.694	115.167	8.207	5950	293.004	193.915	243.459	59,686.1	13,676.9	296.6

where "M_A" denotes the tetrahedral A-site molecular weight and "M_B" is the octahedral B-site molecular weight. The reported values for the force constants K_t and K_o are shown in Table 4. It has been shown that K_t values are higher than K_o values. Table 4 shows that the values of the force constants K_t decrease and K_o increase as the crystallite size increases owing to fluctuations in cation-oxygen bond lengths at the A- and B-site [28].

To determine the conduction mechanism of the tested samples, the Debye temperature D should be calculated as follows [32]:

$$\theta_D = \frac{\hbar \, c \, \nu_{av}}{k_B} \tag{3}$$

$$\nu_{av} = \frac{\nu_t + \nu_o}{2} \tag{4}$$

$$\hbar = \frac{h}{2\pi} \tag{5}$$

where c represents the speed of light (3×10^{10} cm/s), k_B represents the Boltzmann constant, ν_{av} represents the average frequency, h represents the Plank constant, and ν_t and ν_o represent the frequencies of the tetrahedral A-site and the octahedral B-site, respectively. As can be observed, the values of the Debye temperature play a significant role in determining the conduction mechanism of these nanoparticles.

It can be shown that the slightly higher θ_D values occurred from increasing the annealing temperature of the investigated samples. From Anderson's formula [33], we obtained the following formula for calculating the Debye temperature:

$$\theta'_D = \frac{h}{k_B} \times \left(\frac{3N_A}{4\pi V_A} \right)^{\frac{1}{3}} \times V_m \tag{6}$$

$$V_A = \left(\frac{M}{D_x} \right) \Big/ q \tag{7}$$

where V_A stands for the mean atomic volume, M for the molecular weight, q for the number of atoms in one unit of the formula ($q = 7$), and N_A for the Avogadro number. It was found that increasing the annealing temperature of the nanosamples caused an increase in θ'_D. This increase is described according to the increase of mean wave velocity V_m. The equation to compute the bulk modulus B of solids [34] is:

$$B = \frac{1}{3}\left[C_{11} + 2C_{12}\right] \tag{8}$$

where C_{11} and C_{12} are the constants used to measure stiffness. From the following relation [35], it can be shown that there is a linkage between the average force constant K and the stiffness constant C_{11}:

$$K = aC_{11} \tag{9}$$

Also, the values of the longitudinal elastic wave velocity, also known as V_l, the transverse or shear elastic wave velocity, also known as $V_s = V_t$, and the mean elastic wave velocity, known as V_m, are provided by the following relations [36]:

$$V_l = \left(\frac{C_{11}}{D_x}\right)^{1/2} \tag{10}$$

$$V_t = \frac{V_l}{\sqrt{3}} \tag{11}$$

$$V_m = \frac{1}{3}\left[\frac{1}{V_l^3} + \frac{2}{V_s^3}\right]^{1/3} \tag{12}$$

In addition to this, the values of the longitudinal modulus (L), Young's modulus (E), rigidity modulus (G), and Poisson's ratio (σ) may be determined using the following relations [37]:

$$L = D_x V_l^2 \tag{13}$$

$$G = D_x V_s^2 \tag{14}$$

$$\sigma = \frac{L - 2G}{2(L - G)} \tag{15}$$

$$E = (C_{11} - C_{12})(C_{11} + 2C_{12}) \tag{16}$$

All the values of the elastic parameters that were measured on the samples under investigation are shown in Tables 4, 5. Raising the annealing temperature of the investigated samples shows that the values for L, G, B, and E increased. The concept of interatomic bonding may be used to explain this phenomenon. This indicates that the interatomic bonding of the atoms at 900 °C is much stronger than that at room temperature. In addition to this, the values of Poisson's ratio (σ) remain constant by increasing the annealing temperature of the investigated samples ($\sigma = 0.25$), and they are in good agreement with the theory of isotropic elasticity, which had a range that went from − 1 to 0.5 [38]. Finally, studying the mechanical properties of $Ag_{0.5}Cr_{2.5}O_4$ nanoparticles with the ratio of Ag/Cr (1:5) gave more elastic behavior than that of previous work with a ratio of Ag/Cr (1:1) [21]. Moreover, by increasing the annealing temperature of the investigated samples to 900 °C, an enhancement happened in the mechanical properties, especially in the elasticity of the nanosample.

Table 5 Continuation of the elastic parameters of $Ag_{0.5}Cr_{2.5}O_4$ at room temperature and 900 °C

Samples	V_l (m/s)	Vs = Vt (m/s)	Vm m/s	C44 (Gpa)	G (Gpa)	L (Gpa)	σ (unitless)	C12 (Gpa)	E (Gpa)	B (Gpa)	VA (m3)	θ′ D (K)
Room	5624.9	3247.5	3605.4	97.6	97.6	292.7	0.25	54.9	275.3	134.1	3.8	579.4
900 °C	7060.9	4076.6	4525.8	98.9	98.9	296.6	0.25	55.6	279.1	135.9	5.9	627.8

Antimicrobial study

Figure 5a, b illustrates the nanoparticles of the investigated sample $Ag_{0.5}Cr_{2.5}O_4$ nanoparticles at room temperature in vitro. These figures depict Gram-positive, Gram-negative, and fungal microorganisms and the diameters of their inhibition zones, as described in Table 6. This table demonstrates that $Ag_{0.5}Cr_{2.5}O_4$ nanoparticles had

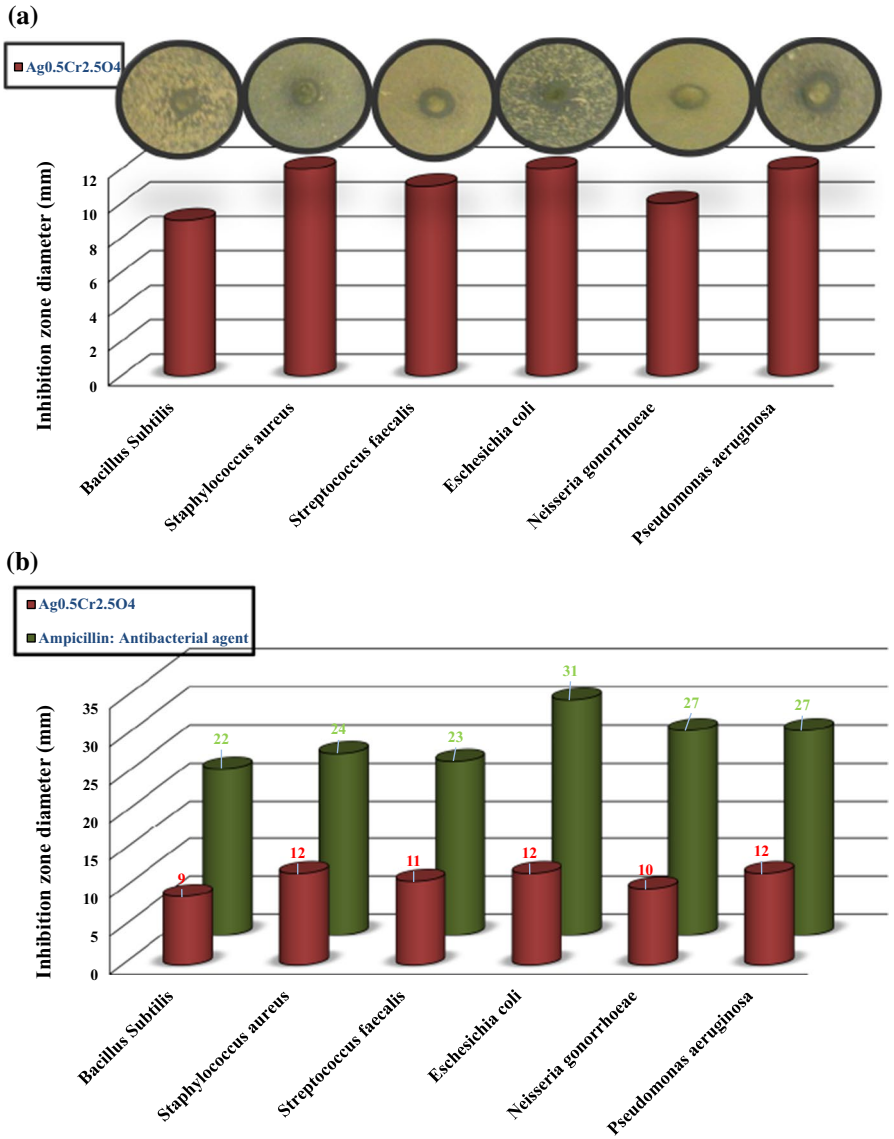

Fig. 5 **a** Antimicrobial diagram of $Ag_{0.5}Cr_{2.5}O_4$ at room temperature. **b** Antimicrobial diagram of $Ag_{0.5}Cr_{2.5}O_4$ at room temperature and ampicillin

Table 6 Inhibition zone parameters values of $Ag_{0.5}Cr_{2.5}O_4$ at room temperature and ampicillin

Samples	Inhibition zone diameter /mm							
	Bacteria						Fungi	
	G +			G −				
	Bacillus subtilis	*Staphylococcus aureus*	*Streptococcus faecalis*	*Escherichia coli*	*Neisseria gonorrhoeae*	*Pseudomonas aeruginosa*	*Aspergillus flavus*	*Candida albicans*
Room	9	12	11	12	10	12	0	0
Ampicillin	22	24	23	31	27	27	0	0
Amphotericin B	0	0	0	0	0	0	16	19

a good antibacterial impact against Gram-positive microbes and Gram-negative microorganisms compared to the antibacterial antibiotic ampicillin. It is observed from Table 6 that the tested bacteria *Staphylococcus aureus*, *Streptococcus faecalis*, and *Pseudomonas aeruginosa* show higher efficacy than the other tested bacteria. When the studied material was added to the tested microorganisms, the cell membrane of the bacteria was disrupted [39–47] due to the presence of toxic silver and chromium ions. Adding $Ag_{0.5}Cr_{2.5}O_4$ nanoparticles, on the other hand, had no impact on fungal germs. Our earlier research [17] showed the antibacterial properties of $Ag_{0.5}Cr_{2.5}O_4$ nanoparticles at 900 °C in detail. Compared to $Ag_{0.5}Cr_{2.5}O_4$ nanoparticles at 900 °C from our previous study [17] and $Ag_{0.5}Cr_{2.5}O_4$ nanoparticles at room temperature from the current work, $Ag_{0.5}Cr_{2.5}O_4$ nanoparticles at 900 °C were stronger against Gram-positive and Gram-negative bacteria than that at room temperature. This may be due to the smaller crystallite size at 900 °C than at room temperature. On the other hand, both samples did not affect the tested fungi. Thus, the investigated samples are highly recommended as an antibacterial agent, particularly against the tested Gram-positive and Gram-negative bacteria.

Conclusion

1. We effectively prepared $Ag_{0.5}Cr_{2.5}O_4$ nanoparticles at various annealing temperatures using a simple and inexpensive technique.
2. The morphology reveals that the crystallite size and particle size of $Ag_{0.5}Cr_{2.5}O_4$ nanoparticles are in the nanoscale range.
3. From the elastic study, $Ag_{0.5}Cr_{2.5}O_4$ nanoparticles at 900 °C showed a higher elasticity than at room temperature.
4. Both samples showed effective behavior against tested Gram-positive and Gram-negative bacteria.
5. $Ag_{0.5}Cr_{2.5}O_4$ nanoparticles at room temperature and 900 °C are innovative materials that have the potential to be incorporated into a variety of medications.

6. In conclusion, the sample $Ag_{0.5}Cr_{2.5}O_4$ nanoparticles at different annealing temperatures are strongly recommended to be applied in biomedical applications.

Author contributions All authors contributed to data analysis, drafting, and revising of the article. All authors read and approved the final manuscript.

Funding Open access funding provided by The Science, Technology & Innovation Funding Authority (STDF) in cooperation with The Egyptian Knowledge Bank (EKB).

Data availability The data that support the findings of this study are available on request from the corresponding author.

Declarations

Conflict of interest The authors declare no conflict of interest.

Ethical approval and consent to participate Not applicable.

Consent for publication Not applicable.

References

1. Honary S, Ghajar K, Khazaeli P, Schalchian P (2011) Preparation, characterization and antibacterial properties of silver-chitosan nanocomposites using different molecular weight grades of chitosan. Trop J Pharm Res 10:69–74
2. Gamal WM, El-Bassuony AAH, Hafez RS, Abdelsalam HK (2022) Study of the structural and magnetic properties of a novel cola/lah nanocomposite material. JOM 74:4898–4908. https://doi.org/10.1007/s11837-022-05491-x
3. Abdelhamid HN, Talib A, Wu H-F (2015) Facile synthesis of water-soluble silver ferrite (AgFeO2) nanoparticles and their biological application as antibacterial agents. RSC Adv 5:34594–34602
4. El-Bassuony AAH, Abdelsalam HK (2019) Tailoring the structural, magnetic and antimicrobial activity of $AgCrO_2$ delafossite at high annealing temperature. J Therm Anal Calorim 138:81–88. https://doi.org/10.1007/s10973-019-08207-7
5. Anooj ES, Sreelekshmi SJ, Gopukumar ST, Praseetha PK (2017) Evaluation of the zinc ferrite nano particles for bio-applications. Int J Pharm Sci Rev Res 46:22
6. Sayed MA, El-Rahman TMAA et al (2022) Attractive study of the antimicrobial, antiviral, and cytotoxic activity of novel synthesized silver chromite nanocomposites. BMC Chem 16:39. https://doi.org/10.1186/s13065-022-00832-y
7. Nangmenyi G, Li X, Mehrabi S, Mintz E, Economy J (2011) Silver-modified iron oxide nanoparticle impregnated fiberglass for disinfection of bacteria and viruses in water. Mater Lett 65:1191

8. Kaskhedikar NA, Maier J (2009) Lithium storage in carbon nanostructures. Adv Mater 21:2664
9. Naseri MG, Saion EB, Ahangar HA, Shaari AH (2013) Fabrication, characterization, and magnetic properties of copper ferrite nanoparticles prepared by a simple, thermal-treatment method. Mater Res Bull 48:1439
10. Li H, Chen Q, Zhao J, Urmila K (2015) Enhancing the antimicrobial activity of natural extraction using the synthetic ultrasmall metal nanoparticles. Sci Rep 5:11033
11. Sayed MA, El-Bassuony AAH, Abdelsalam HK (2020) Evaluation of antimicrobial properties of a novel synthesized nanometric delafossite. Braz J Microbiol 51:1475–1482. https://doi.org/10.1007/s42770-020-00366-2
12. Nomiya K, Yoshizawa A, Tsukagoshi K, Kasuga NC, Hirakawa S, Watanabe J (2004) Synthesis and structural characterization of silver(I), aluminium(III) and cobalt(II) complexes with 4-isopropyltropolone (hinokitiol) showing noteworthy biological activities. Action of silver (I)-oxygen bonding complexes on the antimicrobial activities. J Inorg Biochem 98:46–60
13. El-Bassuony AAH (2020) Effect of Al addition on structural, magnetic, and antimicrobial properties of Ag nanoparticles for biomedical applications. JOM 72:1154–1162. https://doi.org/10.1007/s11837-019-03784-2
14. Huang Z, Jiang X, Guo D, Gu N (2011) Controllable synthesis and biomedical applications of silver nanomaterials. J Nanosci Nanotechnol 11:9395–9408
15. Paulsen JA, Lo CCH, Snyder JE, Ring AP, Jones LL, Jiles DC (2003) Study of the Curie temperature of cobalt ferrite based composites for stress sensor applications. IEEE Trans Magn 39:3316
16. El-Bassuony AAH, Abdelsalam HK (2018) Giant exchange bias of hysteresis loops on Cr3+-doped Ag nanoparticles. J Supercond Novel Magn 31:1539–1544. https://doi.org/10.1007/s10948-017-4340-x
17. El-Bassuony AAH (2020) Influence of high annealing temperature on structural, magnetic and antimicrobial activity of silver chromite nanoparticles for biomedical applications. J Inorg Organomet Polym Mater 30:1821–1828. https://doi.org/10.1007/s10904-019-01306-w
18. El-Ghazzawy EH (2020) Effect of heat treatment on structural, magnetic, elastic and optical properties of the co-precipitated $Co_{0.4}Sr_{0.6}Fe_2O_4$. J Magn Magn Mater 497:166017
19. Rao KS, Kumar AM, Varma MC, Choudary GSVRK, Rao KH (2009) Cation distribution of titanium substituted cobalt ferrites. J Alloys Compd 488:L6
20. Gamal WM, El-Bassuony AH, Abdelsalam HK et al (2021) Role of elastic and optical properties on silver nanoferrite and nanochromite for optical switch device applications. J Mater Sci Mater Electron 32:21590–21602. https://doi.org/10.1007/s10854-021-06667-y
21. El-Bassuony AAH, Abdelsalam HK, Gamal WM (2022) Influence of elastic and optical properties on $AgFeO_2$ and $AgCrO_2$ delafossite to be applied in high-frequency applications. JOM 74:2656–2664. https://doi.org/10.1007/s11837-022-05170-x
22. Bauer AW, Kirby WM, Sherris C, Turck M (1966) Antibiotic susceptibility testing by a standardized single disk method. Am J Clin Pathol 45:493–496
23. Ajroudi L, Mliki N, Bessais L, Madigou V, Villain S, Leroux Ch (2014) Magnetic, electric and thermal properties of cobalt ferrite nanoparticles. Mater Res Bull 59:49
24. Ateia E, El-Bassuony AAH (2017) Fascinating improvement in physical properties of Cd/Co nanoferrites using different rare earth ions. J Mater Sci Mater Electron 28:11482–11490. https://doi.org/10.1007/s10854-017-6944-0
25. El-Bassuony AAH, Abdelsalam HK (2020) Correlation of heat treatment and the impurities accompanying Ag nanoparticles. Euro Phys J Plus 135:66. https://doi.org/10.1140/epjp/s13360-019-00025-y
26. Bouokkeze D, Massoudi J, Hzez W, Smari M, Bougoffa A, Khirouni K, Dhahri E, Bessais L (2019) Investigation of the structural, optical, elastic and electrical properties of spinel $LiZn_2Fe_3O_8$ nanoparticles annealed at two distinct temperatures. RSC Adv 9:40940
27. Albalah MA, Alsabah YA, Mustafa DE (2020) Characteristics of co-precipitation synthesized cobalt nanoferrites and their potential in industrial wastewater treatment. SN Appl Sci 2:804
28. Waldron RD (1955) Infrared spectra of ferrites. Phys Rev 99:1727–1735
29. Mazen SA, Mansour SF, Dhahri E, Zaki HM, Elmosalami TA (2009) The infrared absorption and dielectric properties of Li-Ga ferrite. J Alloy Compd 470:294–300
30. Watawe SC, Sutar BD, Sarwade BD, Chougule BK (2001) Infrared studies of some mixed Li–Co ferrites. Int J Inorg Mater 3:819–823
31. Kuo MF, Hung YH, Huang JY, Huang CC (2016) Structure and magnetic properties of Mn and Al doped magnesium ferrite. China Steel Tech Rep 29:44

32. Modi KB, Trivedi UN, Pandya MP, Bhatu SS, Chhantbar MC, Joshi HH (2004) Microwaves and optoelectronics. Anamaya Publishers, New Delhi
33. Anderson OL (1965) Physical acoustics, vol III. Academic Press, New York
34. Modi KB, Trivedi UN, Pandya MP, Bhatu SS, Chhantbar MC, Joshi HH (2004) Study of elastic properties of magnesium and aluminum co-substituted lithium ferrite near microwave frequencies, in microwaves and optoelectronics. Anamaya Publishers, New Delhi, p 223
35. Ravinder D, Balachander L, Venudhar YC (2001) Elastic behaviour of manganese substituted lithium ferrites. Mater Lett 49:205
36. Patil VG, Shirsath SE, More SD et al (2009) Effect of zinc substitution on structural and elastic properties of cobalt ferrite. J Alloy Compd 488:199–203
37. Raj B, Rajendram V, Palanichamy P (2004) Science and technology of ultrasonics. Narosa Publishing House, New Delhi
38. Modi KB, Rangolia MK, Chhantbar MC, Joshi HH (2006) Study of infrared spectroscopy and elastic properties of fine and coarse grained nickel-cadmium ferrites. J Mater Sci 41:7308–7318
39. El-Bassuony AAH, Gamal WM, Abdelsalam HK (2022) Fascinating study of adding nanocomposite cobalt nano ferrite to silver nanoparticles accompanied magnetite impurity. J Mater Sci Mater Electron 33:16219–16235. https://doi.org/10.1007/s10854-022-08516-y
40. Beyth N, Houri-Haddad Y, Domb A, Khan W, Hazan R (2015) Alternative antimicrobial approach: nano-antimicrobial materials. Evid Based Complement Altern Med 2015:246012. https://doi.org/10.1155/2015/246012
41. Akhtar MN, Saleem M, Khan MA (2018) Al doped spinel and garnet nanostructured ferrites for microwave frequency C and X-band applications. J Phys Chem Solids 123:260
42. El-Bassuony AAH, Abdelsalam HK (2023) Attractive study of the physical properties of silver iron oxide nanoparticles for biomedical applications. Phys Scr 98:055919. https://doi.org/10.1088/1402-4896/acc90c
43. Ali EAM, Sayed MA, Abdel-Rahman TMA, Hussein AM, Hussein R (2019) Bioremediation of waste water from cadmium pollution using silicon dioxide nanoparticles and fungal biomasses. J Pure Appl Microbiol 13:1561–1570. https://doi.org/10.22207/JPAM.13.3.29
44. El-Bassuony AAH, Gamal WM, Abdelsalam HK (2022) Influence of silver nanoferrite and nanochromite on physical properties for high-frequency and biomedical applications. JOM 74:2635–2644. https://doi.org/10.1007/s11837-022-05315-y
45. Baiomy AA (2016) Histopathological biomarkers and genotoxicity in gill and liver tissues of Nile tilapia *Oreochromis niloticus* from a polluted part of the Nile River. Egypt Afr J Aquat Sci 41:181–19127. https://doi.org/10.2989/16085914.2016.1168734
46. El-Bassuony AAH, Gamal WM, Abdelsalam HK (2023) Impact of different magnetic materials added to silver-magnetite nanoparticles on the structural, magnetic and antimicrobial properties. Euro Phys J Spec Top. https://doi.org/10.1140/epjs/s11734-022-00759-4
47. Alkhedaide AQH, Alshehri ZS, Soliman MM, Althumali KW, Abu-Elzahab HS, Baiomy AA (2016) Vitamin D3 supplementation improves immune and inflammatory response in vitamin D deficient adults in Taif, Saudi Arabia. Biomed Res (India) 27:1049–1053